

Phase transition in lithium manganite spinel, LiMn_2O_4 Nobuo Ishizawa^{1,*}, Kenji Tateishi², Katsumi Suda², Douglas du Boulay²,James R. Hester³, Timo P. Vaalsta⁴ and Shunji Kishimoto⁵¹Nagoya Institute of Technology, Tajimi 507-0071, Japan²Tokyo Institute of Technology, Yokohama 226-8503, Japan³Australian Nuclear Science and Technology Organization, New South Wales 2234, Australia⁴University of Western Australia, Western Australia 6009, Australia⁵Photon Factory, Tsukuba 305-0801, Japan

This report summarizes our recent achievements including those given in a paper, “Bond-length fluctuation in the orthorhombic $3\times 3\times 1$ superstructure of the LiMn_2O_4 spinel” by N. Ishizawa, K. Tateishi, S. Oishi and S. Kishimoto, *American Mineralogist* (2014) in press.

1 Introduction

As detailed in our paper [1], the high-temperature form is an AB_2O_4 spinel-type with a normal cationic configuration, where A, B and O are also designated as the tetrahedral and octahedral cation sites and oxygen ion site, having cubic $Fd\bar{3}m$ symmetry with a unit cell dimension $a_c \approx 8.3\text{\AA}$. The low-temperature form crystallizes in orthorhombic $Fddd$ symmetry, having unit cell dimensions along **a** and **b** approximately triple that of the high-temperature prototype. This $3a_c \times 3a_c \times 1a_c$ (abbreviated as $3\times 3\times 1$) superstructure was first identified by a neutron powder diffraction and electron microscopy study [2], and confirmed later by single-crystal synchrotron X-ray diffraction [3].

The phase transition of LiMn_2O_4 accompanies a charge disproportionation of Mn atoms occupying the octahedral B sites of the AB_2O_4 spinel. Since the mean oxidation state of Mn in LiMn_2O_4 is +3.5, the simplest scheme would be a disproportionation into Mn^{3+} and Mn^{4+} in equal fractions. However, the spinel-type structure, where the B-site ions are located at the nodes of a corner-linked tetrahedral network, does not allow alternative charge-ordering topologies, such as $-\text{Mn}^{3+}-\text{Mn}^{4+}-\text{Mn}^{3+}-\text{Mn}^{4+}-$. The structural complexity of the low-temperature LiMn_2O_4 thus arises from frustrated charge disproportionation on the tetrahedral B-site network, which has not been fully solved to date. The present study was undertaken to resolve this problem.

2 Experiment

Preliminary single-crystal diffraction experiments were conducted using a three-circle imaging-plate diffractometer (Rigaku Rapid) with $\text{Mo K}\alpha$ X-rays. The transition was of the first order, having transition points of 294 (1) K during cooling, and 310 (1) K during heating. A preliminary powder X-ray diffraction study on the high-temperature form was performed at beamline 20B (The Australian National Beamline Facility) at the Photon Factory.

Single-crystal synchrotron X-ray diffraction experiments were carried out at beamline 14A at the Photon Factory, using a horizontal-type four-circle

diffractometer [4, 5]. The sample was first warmed, using a nitrogen gas stream, to 320 K, at which point the data collection was carried out over three days. The sample was then cooled at a rate of 2 K min^{-1} to 230 K, at which point another data collection was carried over four days. Cell dimensions were calculated at these temperatures from 24 reflections at $2\theta \approx 86^\circ$. The cooling procedure from 320 to 230 K was interrupted several times in order to calculate cell dimensions at intermediate temperatures of 300, 280, and 250 K, using 12 reflections at $2\theta \approx 86^\circ$ and $2\theta \approx 66^\circ$.

Intensity data were collected for the hemisphere of reciprocal space in the range $1^\circ < 2\theta < 100^\circ$ at 230 K, and the full sphere in the range $1^\circ < 2\theta < 130^\circ$ at 320 K. An *F* lattice centering was assumed for both data collections according to the previous study [3]. An eight-channel avalanche photodiode detector [6], possessing a large dynamic range (up to $\sim 5 \times 10^8$ cps) for the X-rays employed allowed for the elimination of all the attenuators and absorbers along the X-ray path. The wavelength of the X-rays emitted from the vertical wiggler was calibrated using a silicon single crystal to be 0.75064\AA at 230 K and 0.75059\AA at the other temperatures, including 320 K.

The crystallography program packages, Xtal [7] and Jana2006 [8], were used for data processing and structure refinement, respectively. The anomalous scattering factors and the X-ray absorption coefficients at the experimental wavelength were taken from the Sasaki tables [9, 10].

3 Results and Discussion

The orthorhombic $3\times 3\times 1$ superstructure of the low-temperature form has a network of Mn^{4+} ions at the vertices of a slightly distorted truncated square tessellation comprising one square and two octagonal prisms as shown in Fig. 1. The square prism and one type of octagonal prism house Mn^{3+} ions with Jahn–Teller (JT) elongated Mn–O bonds almost parallel to the *c* and *b* axes, respectively, whereas the other octagonal prism houses Mn ions with JT-induced bond-length fluctuation for the Mn–O bonds lying almost parallel to the *a* axis.

The Mn ions in the latter octagonal prism (Mn2 among crystallographically independent Mn1–Mn5 sites) are assumed to exchange their oxidation states dynamically between 3+ and 4+ in a time ratio of ~3:1, forming a polaron centered at a Mn_4O_4 heterocubane cluster with orbital and spin orders.

The bond-length fluctuation results from an exchange in oxidation states of Mn2 between 3+ and 4+, because Mn^{3+} in a high-spin state electronic configuration ($t_{2g}^3 e_g^1$) is stabilized in the Jahn–Teller (JT) elongated tetragonal dipyramid, whereas Mn^{4+} ($t_{2g}^3 e_g^0$) is stabilized in a relatively regular coordination octahedron.

The present study favors the structure model for the $1 \times 1 \times 1$ high-temperature form [11], in which the oxygen ions are distributed statically at the Wyckoff 96g site of the space group $Fd\bar{3}m$, in contrast with the widely used model that assumes the oxygen ions lie at the 32e site. However, it should be noted that even the 96g model has a drawback in fully explaining the disordered distribution of Mn–O distances: an alternative model assuming the anharmonic vibration of oxygen ions, is proposed in our paper [1].

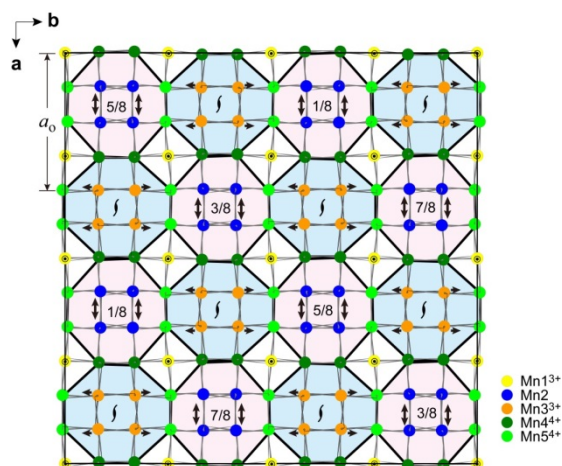


Fig. 1: The geometrical arrangement of Mn atoms in the orthorhombic $3 \times 3 \times 1$ $Fddd$ supercell of the LiMn_2O_4 spinel viewed along c (After Ishizawa et al., 2014, [1]). The JT-inactive Mn^{4+} and Mn^{5+} lie at the vertices of a slightly distorted network of a truncated square tessellation, composed of square and octagonal prisms. The square prism (white) houses Mn1 with JT distortion along c (perpendicular to the paper), the octagonal prism (pink) houses the Mn_2O_9 heterocubane with the JT-induced bond-length fluctuation along a , and the other octagonal prism (blue) houses Mn3 with the JT distortion along b . The directions of JT distortions are given by small arrows. The a -length of the prototype spinel is shown as a_0 . The z -heights of the Mn_2O_9 heterocubane center are given as $1/8$, $3/8$, etc.

In the $3 \times 3 \times 1$ superstructure of LiMn_2O_4 , the molecular polaron is centred only at the Mn_2O_9 heterocubane. The polarons are confined in one type of the octagonal prism in the truncated square tessellation of Mn^{4+} ions with spin states opposite to that of Mn2. Since the high-temperature form of LiMn_2O_4 has a cubic unit cell of the spinel-type, manganese atoms are expected to have spin and orbital freedoms. The spin blockade achieved by the formation of the truncated square tessellation is broken in the high-temperature form, allowing a free migration of polarons. The cubic–orthorhombic phase transition of LiMn_2O_4 near room temperature can thus be regarded as an order–disorder transition of the molecular polarons centred at the Mn_4O_4 heterocubanes.

Acknowledgement

Crystals were grown by Prof. S. Oishi, Faculty of Engineering, Shinshuu University. The synchrotron experiments were performed based on the programs 2002G042, 2006G242, 2009G005 and 2011G022. This work was supported by JSPS KAKENHI Grant numbers 18206071 (2006–2008) and 22360272 (2010–2013).

References

- [1] N. Ishizawa et al., *Am. Mineral.*, 99 (2014), 1528–1536. DOI: <http://dx.doi.org/10.2138/am.2014.4840>.
- [2] Rodríguez-Carvajal et al., *Phys. Rev. Lett.* 81, 4660–4663 (1998).
- [3] Tateishi, K. et al., *Acta Cryst.* E60, i18–i21(2004).
- [4] Satow, Y., and Iitaka, Y., *Rev. Sci. Instrum.* 60, 2390–2393, (1989).
- [5] Vaalsta, T.P. and Hester, J.R. (1997) *Diff14A Software*. Photon Factory, KEK, Tsukuba, Japan.
- [6] Kishimoto, S. et al., *Rev. Sci. Instrum.* 69, 384–391 (1998).
- [7] Hall, S. et al., *Gnu Xtal System*. <http://xtal.sourceforge.net> (2002).
- [8] Petricek, V. et al., *Jana2006, Structure Determination Software Programs*, Institute of Physics, Praha, Czech Republic (2006)
- [9] Sasaki, S., *KEK Report*, 88-14, 1-136 (1989).
- [10] Sasaki, S., *KEK Report* 90-16, 1-143 (1990).
- [11] Takahashi, Y. et al., *J. Phys. Soc. Japan* 72, 1483–1490 (2003).

* ishizawa@nitech.ac.jp